Front. Earth Sci. 2016, 10(1): 159–170
DOI 10.1007/s11707-015-0497-4

RESEARCH ARTICLE

Source of atmospheric moisture and precipitation over China's major river basins

Tongtiegang ZHAO (✉), Jianshi ZHAO, Hongchang HU, Guangheng NI

State Key Laboratory of Hydro-Science and Engineering, Department of Hydraulic Engineering, Tsinghua University, Beijing 100084, China

Abstract Oceanic evaporation via the East Asian Monsoon (EAM) has been regarded as the major source of precipitation over China, but a recent study estimated that terrestrial evaporation might contribute up to 80% of the precipitation in the country. To explain the contradiction, this study presents a comprehensive analysis of the contribution of oceanic and terrestrial evaporation to atmospheric moisture and precipitation in China's major river basins. The results show that from 1980 to 2010, the mean annual atmospheric moisture (precipitable water) over China was 13.7 mm, 39% of which originates from oceanic evaporation and 61% from terrestrial evaporation. The mean annual precipitation was 737 mm, 43% of which originates from oceanic evaporation and 57% from terrestrial evaporation. Oceanic evaporation makes a greater contribution to atmospheric moisture and precipitation in the East Asian Monsoon Region in South and East China than terrestrial evaporation does. Particularly, for the Pearl River and southeastern rivers, oceanic evaporation contributes approximately 65% of annual precipitation and more than 70% of summer precipitation. Meanwhile, terrestrial evaporation contributes more precipitation in northwest China due to the westerly wind. For the northwestern rivers, terrestrial evaporation from the Eurasian continents contributes more than 70% of precipitation. There is a linear relation between mean annual precipitation and the contribution of oceanic evaporation to precipitation, with a correlation coefficient of 0.92, among the ten major river basins in China.

Keywords oceanic evaporation, terrestrial evaporation, moisture transport, East Asian Monsoon, westerly wind, Tibetan Plateau

Received July 10, 2014; accepted September 15, 2014

E-mail: zttg@mail.tsinghua.edu.cn

1 Introduction

Precipitation results from moisture in over-saturated air. This moisture originates from either oceanic or terrestrial evaporation as part of the global water cycle's continuous transport of water among land, ocean, and atmosphere. Globally, approximately 10% of oceanic evaporation is transported to land and contributes about 40% of terrestrial precipitation (Oki and Kanae, 2006; Trenberth et al., 2007; Gimeno et al., 2010). However, the contribution of oceanic evaporation to precipitation over land varies considerably across the globe (Keys et al., 2012; Xu et al., 2013; van der Ent and Savenije, 2013). For example, the North Atlantic Subtropical Ocean exhibits an extensive influence: its evaporation contributes to precipitation over large parts of Eurasia, Mexico, and even South America. In contrast, the South Pacific and Indian Oceans provide a moisture source for Australia and Indonesia (Gimeno et al., 2012). Precipitation over different regions has different sources. For example, northern Europe and eastern North America receive moisture from evaporation in the Northern Hemisphere, whereas northern South America receives moisture from both the Northern and Southern hemispheres (Gimeno et al., 2010).

The source of atmospheric moisture and precipitation has been an important issue in the global water cycle. It reveals the teleconnections between atmospheric circulation and regional precipitation, and also helps to develop seasonal predictions of precipitation from climatic indices (Liu et al., 2012; Wei et al., 2012; Chen and Chen, 2014). For example, given the contribution of evaporation originating from the North Atlantic Ocean to precipitation over the adjacent continents, accurate characterization of the North Atlantic Oscillation improves prediction of seasonal precipitation in North America and Europe (Wilby et al., 2004; Gimeno et al., 2012). A recent study illustrated that the North Atlantic Oscillation even affects

weather in northeast China due to its triggering effect on the high-level tropospheric Rossby wave in the Eurasian continent (Zhou et al., 2013). Moreover, exploring the source of atmospheric moisture facilitates understanding of the vulnerability of rainfall-dependent regions to atmospheric perturbations, and can help to improve water resources management policies (Keys et al., 2012; van der Ent and Savenije, 2013).

Regarding the source of precipitation over China, it is conventionally recognized that oceanic evaporation represents the major source of atmospheric moisture and precipitation for China's major river basins. This concept is based on the East Asian Monsoon (EAM) that plays a significant role and delivers atmospheric moisture originating from the Indo-China Peninsula, South China Sea, and Pacific Ocean to China (Ding and Chan, 2005; Huang and Chen, 2010; Li et al., 2011). However, a recent study (van der Ent et al., 2010) based on a water accounting model, estimated that due to the effect of the westerly wind, up to 80% of precipitation in China originates from evaporation from the Eurasian continents. This striking conclusion contradicts the results of the EAM studies. However, the focus of the EAM studies is on atmospheric wind circulations that determine atmospheric moisture and precipitation in East Asia, and the contributions of oceanic and terrestrial evaporation are not quantified. This study attempts to explain the contradiction based on a comprehensive analysis of the source of atmospheric moisture and precipitation over China. The purpose of this study is three-fold: 1) quantify the contributions of oceanic and terrestrial evaporation to atmospheric moisture and precipitation over China, 2) analyse the spatial variation of the contributions across China's ten major river basins, and 3) discuss the connections between the atmospheric moisture, precipitation sources, and atmospheric circulation patterns, particularly the EAM and the westerly wind.

The remainder of the paper is organized in the following manner: Section 2 illustrates the model and data used in the analysis; Section 3 conducts a validation and examines performances of the model; Section 4 presents an analysis of the source of atmospheric moisture (precipitable water) over China; Section 5 illustrates the source of precipitation and explores the effect of atmospheric circulation patterns; and Section 6 contains the summary.

2 Water accounting model

This study sets up a global water accounting model (van der Ent et al., 2010; van der Ent and Savenije, 2011) driven by the ERA-Interim reanalysis data (Dee et al., 2011) to analyse the source of atmospheric moisture and precipitation over China. The water accounting model is essentially a water balance model that treats the globe as a grid of columns separated by lines of latitude and longitude. Accounting for moisture fluxes within and between columns, the model analyses the movement of atmospheric moisture from a certain region in the context of the balance of global atmospheric moisture.

Global atmospheric moisture balance lays the basis for the accounting analysis:

$$\frac{\partial s_a}{\partial t} + \frac{\partial (s_a u)}{\partial x} + \frac{\partial (s_a v)}{\partial y} = E - P, \tag{1}$$

in which s_a denotes the total atmospheric moisture storage, and $\frac{\partial s_a}{\partial t}$ represents changing rate of atmospheric moisture. u and v respectively represent zonal and meridional wind speeds, and $\frac{\partial (s_a u)}{\partial x}$ and $\frac{\partial (s_a v)}{\partial y}$ are changing rates of horizontal water fluxes in the west-east and south-north directions, respectively. E and P are the surface evaporation and precipitation, which are the source and sink of atmospheric moisture, respectively. Eq. (1) explicitly includes the three dimensions of latitude, longitude, and time. In addition, there is an implicit fourth dimension: pressure level. Specific humidity and wind speed vary at different pressure levels. Atmospheric moisture and horizontal fluxes are calculated at each pressure level and then vertically integrated.

Indices for latitude, longitude, pressure level, and time are denoted as i, j, k, and t, respectively. The total atmospheric moisture s_a in grid column (i, j) at time step t is calculated as follows:

$$s_a|_{(i,j,t)} = \frac{1}{\rho_w g} \sum_k \left[\frac{q(i,j,k,t) + q(i,j,k+1,t)}{2} \times \Big(p(k+1) - p(k) \Big) \right]. \tag{2}$$

In Eq. (2), q represents specific humidity (mass of water vapour in a unit mass of moist air); p denotes pressure level; ρ_w indicates density of water, i.e., 1,000 kg/m^3; and g is the acceleration of gravity, 9.8 N/kg. The equation represents numerical vertical integration of $s_a = \frac{1}{\rho_w g} \int_{p=0}^{p_s} q \mathrm{d}p$, in which p_s denotes surface pressure. The unit of $s_a|_{(i,j,t)}$ is m.

$\frac{\partial (s_a u)}{\partial x}$ and $\frac{\partial (s_a v)}{\partial y}$ are also derived through numerical integration. Denoting $F_{W-E}(i,j,t)$ and $F_{S-N}(i,j,t)$ respectively as zonal and meridional fluxes at grid column (i, j) at time step t, the fluxes are calculated as follows:

$$\begin{cases} F_{W-E}(i,j,t) = \dfrac{w}{\rho_w g}\sum\limits_k \left[\dfrac{q(i,j,k,t)+q(i,j,k+1,t)}{2} \right. \\ \qquad \left. \times \dfrac{u(i,j,k,t)+u(i,j,k+1,t)}{2} \times \Big(p(k+1)-p(k)\Big)\right] \\ F_{S-N}(i,j,t) = \dfrac{w}{\rho_w g}\sum\limits_k \left[\dfrac{q(i,j,k,t)+q(i,j,k+1,t)}{2} \right. \\ \qquad \left. \times \dfrac{v(i,j,k,t)+v(i,j,k+1,t)}{2} \times \Big(p(k+1)-p(k)\Big)\right] \end{cases}. \tag{3}$$

In Eq. (3), w denotes the width of the grid column under analysis. Notably, when calculating zonal flux $F_{W-E}(i,j,t)$, w represents the column's width along the longitude line, which is constant; when calculating meridional flux $F_{S-N}(i,j,t)$, w is the width across the latitude line, which varies with latitude. The unit of $F_{W-E}(i,j,t)$ and $F_{S-N}(i,j,t)$ is m^3/s. Based on the flux variables, $\frac{\partial(s_a u)}{\partial x}$ and $\frac{\partial(s_a v)}{\partial y}$ in grid column (i, j) during time step t are derived:

$$\begin{cases} \left.\dfrac{\partial(s_a u)}{\partial x}\right|_{(i,j,t)} = \dfrac{\Delta t}{A}[F_{W-E}(i-1,j,t)-F_{W-E}(i+1,j,t)] \\ \left.\dfrac{\partial(s_a v)}{\partial y}\right|_{(i,j,t)} = \dfrac{\Delta t}{A}[F_{S-N}(i,j-1,t)-F_{S-N}(i,j+1,t)] \end{cases}. \tag{4}$$

In Eq. (4), Δt denotes the length of time step, in second, and A represents the bottom area of the grid column, in m^2. The unit of $\frac{\partial(s_a u)}{\partial x}$ and $\frac{\partial(s_a v)}{\partial y}$ is m. Eq. (4) is incorporated into Eq. (1). As can be seen, fluxes to and from adjacent columns lead to change of atmospheric moisture in one grid column.

The above equations illustrate the balance of global atmospheric moisture. In the context of global moisture balance, the water accounting model investigates the movement of atmospheric moisture that originates from a certain region. The study region is denoted as Ω and atmospheric moisture originating from Ω as s_{a_Ω}. Similar to Eq. (1), movement of s_{a_Ω} is formulated as:

$$\frac{\partial s_{a\_\Omega}}{\partial t} + \frac{\partial(s_{a\_\Omega} u)}{\partial x} + \frac{\partial(s_{a\_\Omega} v)}{\partial y} = E_{a\_\Omega} - P_{a\_\Omega}. \tag{5}$$

In Eq. (5), the left-hand side indicates movement of s_{a_Ω}; at the right-hand side, evaporation E_{a_Ω} and precipitation P_{a_Ω} represent source and sink of s_{a_Ω}, respectively. It is important to note that Ω in E_{a_Ω} can be set as ocean or land. When the grid column is inside Ω, E_{a_Ω} is set as the original evaporation value of E (Eq. (1)); otherwise, E_{a_Ω} is set as zero. This setting facilitates a flexible approach to analysing movement of moisture originating from Ω.

The "well-mixed" assumption has been made to analyse s_{a_Ω} (van der Ent et al., 2010):

$$\frac{s_{a\_\Omega}}{s_a} = \frac{P_{a\_\Omega}}{P} = \frac{\dfrac{\partial(s_{a\_\Omega} u)}{\partial x}}{\dfrac{\partial(s_a u)}{\partial x}} = \frac{\dfrac{\partial(s_{a\_\Omega} v)}{\partial y}}{\dfrac{\partial(s_a v)}{\partial y}}. \tag{6}$$

The implications of Eq. (6) are that E_{a_Ω} is mixed with moisture already in the grid column once it enters the column and that the ratio of moisture originating from Ω is the same for moisture storage and fluxes. By transforming the equation, the following is derived:

$$\begin{cases} P_{a\_\Omega} = \dfrac{s_{a\_\Omega}}{s_a} P \\ \dfrac{\partial(s_{a\_\Omega} u)}{\partial x} = \dfrac{s_{a\_\Omega}}{s_a}\dfrac{\partial(s_a u)}{\partial x} \\ \dfrac{\partial(s_{a\_\Omega} v)}{\partial y} = \dfrac{s_{a\_\Omega}}{s_a}\dfrac{\partial(s_a v)}{\partial y} \end{cases}. \tag{7}$$

Incorporating Eq. (7) into Eq. (5), we have

$$\frac{\partial s_{a\_\Omega}}{\partial t} + \frac{s_{a\_\Omega}}{s_a}\frac{\partial(s_a u)}{\partial x} + \frac{s_{a\_\Omega}}{s_a}\frac{\partial(s_a v)}{\partial y} = E_{a\_\Omega} - \frac{s_{a\_\Omega}}{s_a} P. \tag{8}$$

In Eq. (8), s_a, $\frac{\partial(s_a u)}{\partial x}$, and $\frac{\partial(s_a v)}{\partial y}$ are derived in Eqs. (1) to (4); E_{a_Ω} and P are from global dataset (van der Ent et al., 2010; Dee et al., 2011). As can be seen, s_{a_Ω} is supplemented by evaporation E_{a_Ω}, conveyed by horizontal fluxes $\frac{s_{a\_\Omega}}{s_a}\frac{\partial(s_a u)}{\partial x}$ and $\frac{s_{a\_\Omega}}{s_a}\frac{\partial(s_a v)}{\partial y}$, and depleted by precipitation $\frac{s_{a\_\Omega}}{s_a} P$. The movement of atmospheric moisture s_{a_Ω} that originates from Ω is simulated (Eq. 8) along with the global water vapour transport (Eq. 1).

Based on s_{a_Ω} and s_a, the contribution of evaporation from Ω to atmospheric moisture over region R is derived using the "well-mixed" assumption (Eqs. (6) and (7)),

$$C_{\text{moisture}} = \frac{\sum\limits_{(i,j)\in R} s_{a\_\Omega}}{\sum\limits_{(i,j)\in R} s_a}. \tag{9}$$

The contribution of evaporation from Ω to precipitation over region R is estimated as follows

$$C_{\text{precipitation}} = \frac{\sum_{(i,j)\in R} \frac{s_{a\_\Omega}}{s_a} P}{\sum_{(i,j)\in R} P}. \quad (10)$$

To summarize, the water accounting model requires the following input data: surface pressure p_s, specific humidity q, zonal wind speed u, meridional wind speed v, evaporation E, and precipitation P. There are four dimensions for these data, including latitude, longitude, pressure level, and time. The input data are retrieved from the ERA-Interim re-analysis dataset that assimilates information from multiple observational and remote sensing data sources (Gevorgyan, 2013; Sun and Wang, 2013). The ERA-Interim dataset provided by the European Center for Medium-range Weather Forecasts (ECMWF, http://apps.ecmwf.int/datasets/) covers the period from 1979 through the present. Thirty-two years of data from 1979 to 2010 are used in the analysis. Following the model setup in van der Ent et al. (2010), we analyse the area between latitudes 57°S and 79.5°N, which covers all continents except Antarctica. Note that, the data for q, u, and v are retrieved from 24 pressure levels between 175 hPa and 1,000 hPa. Table 1 provides a description of the data.

The data processing is briefly summarized in Fig. 1. To run the water accounting model, surface pressure, specific humidity, and zonal and meridional wind speed are used in numerical vertical integration to derive the total atmospheric moisture (Eq. (2)) and horizontal fluxes (Eqs. (3) and (4)), for which the temporal resolution is 6-hour. Secondly, for the sake of numerical stability, temporal resolution of atmospheric moisture and horizontal fluxes, as well as evaporation and precipitation, is disaggregated into 0.5-hour ($\Delta t = 1{,}800$ seconds (Eq. 4)) intervals (van der Ent et al., 2010; van der Ent and Savenije, 2011). The 0.5-hour atmospheric data forms the basis for the simulation of the balance of global atmospheric moisture (Eq. (1)) and the movement of atmospheric moisture originating from a certain region (Eq. (8)). Using the total atmospheric moisture and moisture from a certain region, contributions of evaporation from that region to atmospheric moisture and precipitation in other regions are quantified. This study focuses on the contribution of oceanic and terrestrial evaporation to atmospheric moisture and precipitation over the ten major river basins in China.

3 Examination of the water accounting model

Before analysing the source of atmospheric moisture and precipitation for China, we employ the global ERA-Interim

Table 1 Input data of the water accounting model

Name	Symbol	Temporal resolution	Unit	Dimension
Surface pressure	p_s	6-hour	Pa	Latitude, longitude, time
Specific humidity	q	6-hour	kg/kg	Latitude, longitude, time, pressure level
Zonal wind speed	u	6-hour	m/s	Latitude, longitude, time, pressure level
Meridional wind speed	v	6-hour	m/s	Latitude, longitude, time, pressure level
Evaporation	E	6-hour	m	Latitude, longitude, time
Precipitation	P	6-hour	m	Latitude, longitude, time

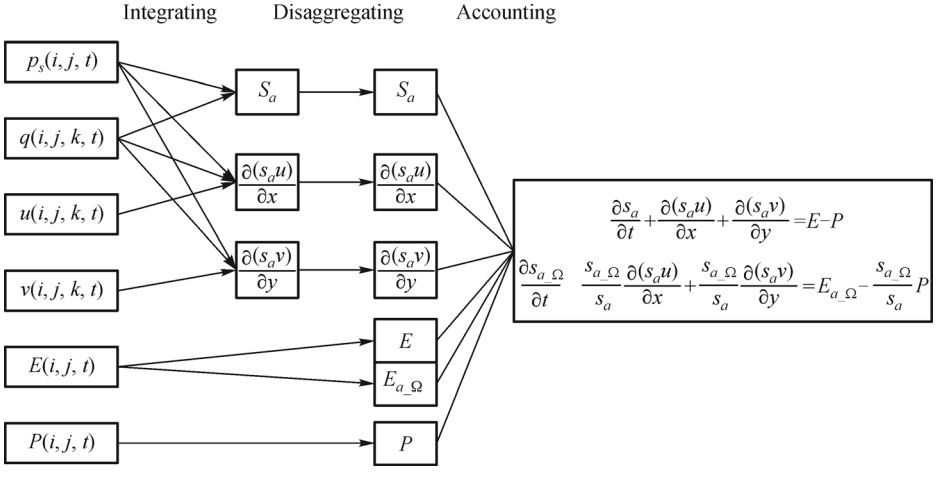

Fig. 1 Schematic of the structure of the water accounting model.

re-analysis data (Dee et al., 2011) and examine the water accounting model's performances from a global perspective. Re-analysis data generated by assimilation of observational and remote sensing data provides a reliable representation of the global water cycle (Gevorgyan, 2013; Sun and Wang, 2013). Treating ERA-Interim data as perfect, the procedure of examination is as follows: 1) the study region Ω is set as the ocean and transport of moisture originating from oceanic evaporation is analysed. The water accounting model runs from 1979 to 2010. The initial atmospheric moisture originating from the ocean at 0:00 January 1, 1979 is set as 0 mm (notably, the unit of moisture is m in the computation, and it is converted into mm for the sake of illustration in result analysis), and the whole year of 1979 is used to spin-up the model. The annual mean atmospheric moisture originating from the ocean during 1980 to 2010 is presented in Fig. 2(a). 2)By setting the study region Ω as the land, the atmospheric moisture originating from the land is then simulated from 1979 to 2010, as shown in Fig. 2(b). 3) Adding up moisture originating from ocean and land, total atmospheric moisture is derived (Fig. 2(c)) and compared to the ERA-Interim reanalysis atmospheric moisture data (Fig. 2(d)).

The simulated moisture is in accordance with the re-analysed moisture across the globe. The gap between simulated and re-analysed moisture (Fig. 2(e)) is small, which indicates the efficiency of the model in investigating the balance of global atmospheric moisture. Meanwhile, some small differences are observed near 57°S and 79.5°N, the boundaries of the study area. The differences are due to the model setting that treats atmospheric moisture transport at the boundary as zero. Figure 2 generally shows that the water accounting model efficiently simulates the balance of global atmospheric moisture from oceanic and terrestrial evaporation. Given that China is located south of 55°N, the contributions of oceanic and terrestrial evaporation to atmospheric moisture over China can be reliably quantified. The examination treats ERA-Interim data as perfect, but there can be some bias depending on the area under

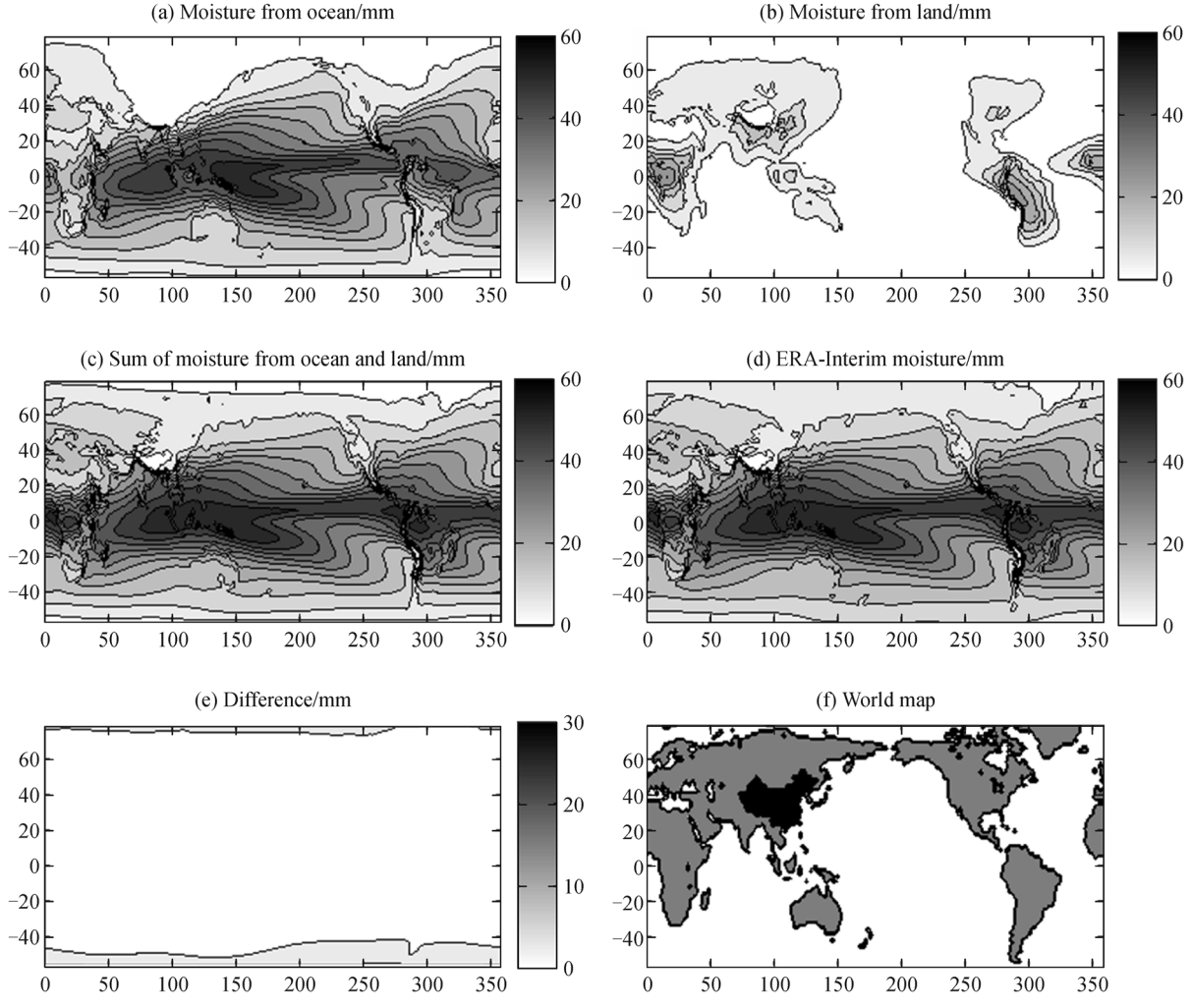

Fig. 2 The mean annual global water balance based from the water accounting model.

investigation (Zhao et al., 2012; Gevorgyan, 2013). Considering possible bias in re-analysis data, the values of atmospheric moisture and the contributions of oceanic and terrestrial evaporation may not be exact, but are reasonable (van der Ent et al., 2010; van der Ent and Savenije, 2011; Keys et al., 2012).

The water accounting model partitions the total atmospheric moisture into two parts, originating from ocean and land. Some interesting observations can be made based on Figs. 2(a) and 2(b). Moisture originating from the ocean spreads extensively across the globe, except for the central Asian and Tibetan Plateau. Near the equator, the moisture exhibits a maximum value, which is up to 60 mm, and it generally decreases as latitude increases. This phenomenon is caused by the reduction in sea surface temperature with increasing latitude. In comparison, atmospheric moisture originating from the land concentrates over continents. As shown in Fig. 2, distribution of atmospheric moisture is also affected by topography. The Rocky Mountains in North America, the Andes Mountains in South America, and the Great Rift Valley in Africa exhibit remarkable blocking effects. Atmospheric moisture on the eastern and western sides of the mountains exhibits drastic changes. The Himalayan Mountains and the Tibetan Plateau exhibit significant influences on atmospheric moisture over East and South Asia.

4 Source of atmospheric moisture

Based on the analysis of global atmospheric moisture, we explore the source of atmospheric moisture over China. In hydrology, atmospheric moisture is also called precipitable water, which indicates the depth of water in a column of atmosphere. The annual mean atmospheric moisture over China from 1980 to 2010 is shown in the upper part of Fig. 3. As can be seen, the moisture over Southeast China has a high value of approximately 40 mm, whereas the moisture over Northwest China is generally below 10 mm. Compared with Fig. 2, Figure 3 illustrates the effects of the Tibetan Plateau in more detail. Atmospheric moisture changes dramatically at the southern and eastern edges of the plateau due to the drastic increase in the altitude of the Himalayan Mountains. To the east of the plateau, atmospheric moisture over East China decreases from south to north; to the north of the plateau, atmospheric moisture over Northwest China is at a low level. The contribution (in percentage) of oceanic evaporation to atmospheric moisture is presented in the lower part of Fig. 3. The humid regions in South and East China receive a greater portion of moisture from oceanic evaporation. On the other hand, the dry regions in Northwest China get a higher percentage of their moisture from terrestrial evaporation in the Eurasia Continent. The Tibetan Plateau exhibits remarkable blocking effects on moisture over China. As illustrated in Fig. 3, owing to the high altitude, atmospheric moisture

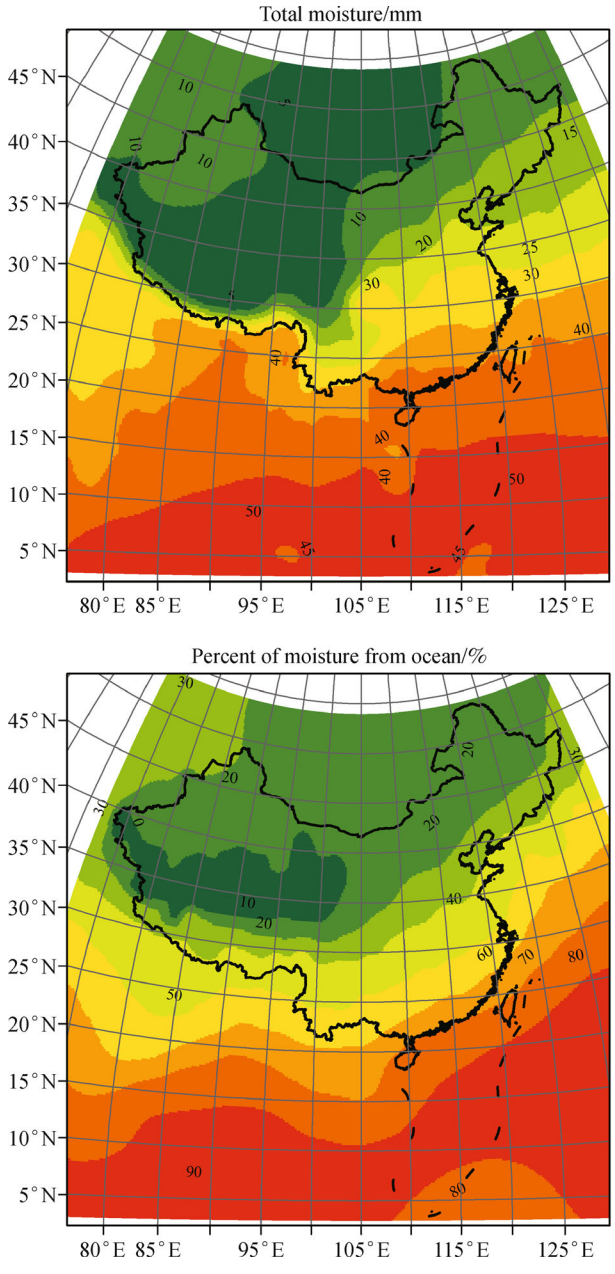

Fig. 3 Mean annual atmospheric moisture over China (from 1980 to 2010) and the contribution of oceanic evaporation.

originating from the ocean can hardly pass over the plateau and reach Northwest China.

Besides topography, the distribution of atmospheric moisture is closely related to atmospheric circulation patterns in China. To the east of the Tibetan Plateau, the climate in East China is dominated by the EAM (Wang and Lin, 2002; Huang and Chen, 2010). The EAM commences over the regions from the Indochina Peninsula and the South China Sea and delivers large amounts of oceanic evaporation northward and northeastward to East China, Korea, and Japan (Ding and Chan, 2005; Huang and Chen, 2010; Li et al., 2011). On the other hand, the westerly wind

dominates the climate in Northwest China. The significant influence of the westerly wind on moisture fluxes in the Eurasia Continent has been illustrated in van der Ent et al. (2010). Due to this influence, atmospheric moisture in Northwest China mainly originates from evaporation in the Eurasian continent. Moreover, it is observed that the EAM and westerly winds interact and jointly affect the atmospheric moisture in Northeast China, where the atmospheric moisture and the contribution of oceanic evaporation tend to decrease from the southeast to the northwest. Figure 3 highlights the effects of the EAM and the westerly wind. These two atmospheric circulation patterns are influenced by the Tibetan Plateau (Ding and Chan, 2005; Qian et al., 2009).

Using the water accounting model, contributions of oceanic and terrestrial evaporation to atmospheric moisture over the 10 major river basins in China (location map is provided in Fig. 4) are evaluated, as shown in Table 2 and Fig. 5. On the whole, the annual mean atmospheric moisture over China is 13.7 mm, of which 39% originates from the ocean and 61% from land. Atmospheric moisture exhibits the highest value in South and East China, known as the East Asian Monsoon Region (Ding and Chan, 2005; Qian et al., 2009), including the Pearl River, southeastern rivers, and the Yangtze and Huai Rivers. Oceanic evaporation contributes up to 50% of the atmospheric moisture in this region. Particularly, the contribution of oceanic evaporation is 62% for the Pearl River and the southeastern rivers. In contrast, terrestrial evaporation makes a greater contribution to atmospheric moisture in Northwest China owing to the prevailing effect of the westerly wind and the blocking effect of the Tibetan Plateau.

The ten major river basins are ranked by the contribution of oceanic evaporation in descending order, as follows: the Pearl River (62%), the southeastern rivers (62%), the Yangtze River (44%), the southwestern rivers (43%), the Huai River (41%), the Liao River (30%), the Hai River (28%), the Songhua River (27%), the Yellow River (25%), and the northwestern rivers (25%). As can be seen, oceanic and terrestrial evaporation contribute to atmospheric moisture in China with considerable spatial differences. The contribution of oceanic evaporation is over 60% for the Pearl River and the southeastern rivers due to the EAM. The Yellow River and the northwestern rivers are located inland. The climate therein is dominated by the westerly wind, and the rivers receive a larger portion of atmospheric moisture (over 70%) from terrestrial evaporation.

5 Sources of precipitation

Based on the analysis of the source of atmospheric moisture, this study also investigates the source of

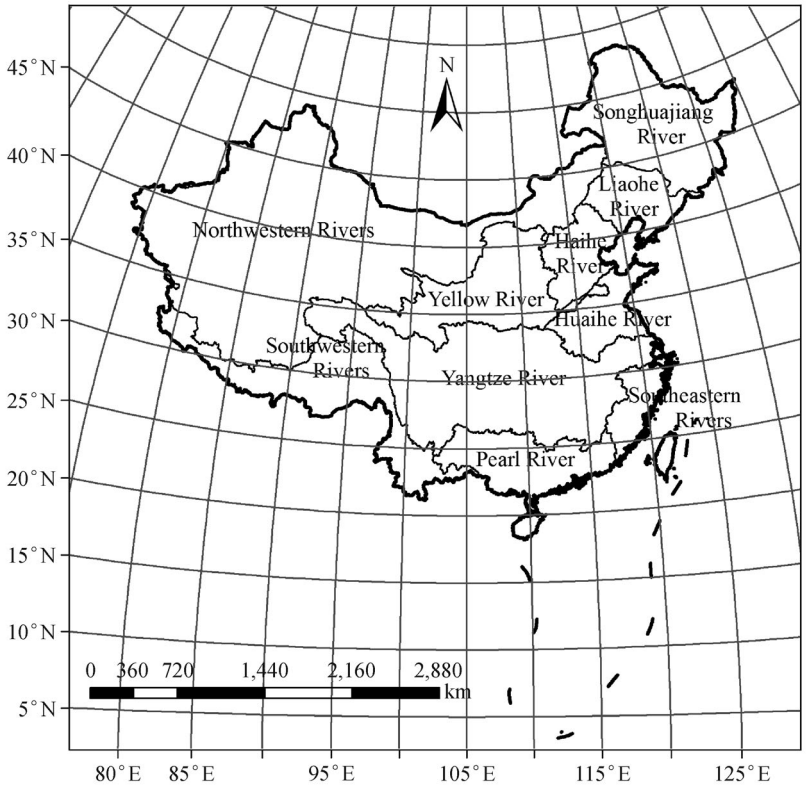

Fig. 4 Location map of the ten major river basins in China.

Table 2 Contribution of oceanic and terrestrial evaporation to atmospheric moisture over China

Location	Moisture originating from the ocean /mm	Moisture originating from the land /mm	Total moisture / mm	% from oceanic evaporation	% from terrestrial evaporation
Songhua River	3.1	8.5	11.6	27	73
Liao River	4.2	9.8	14.0	30	70
Northwestern Rivers	1.8	5.2	7.0	25	75
Hai River	4.1	10.7	14.8	28	72
Yellow River	2.7	8.1	10.8	25	75
Huai River	9.9	14.2	24.0	41	59
Yangtze River	9.6	12.4	22.1	44	56
Southeastern Rivers	19.8	12.3	32.1	62	38
Southwestern Rivers	4.5	5.9	10.4	43	57
Pearl River	21.9	13.4	35.3	62	38
China	5.3	8.3	13.7	39	61

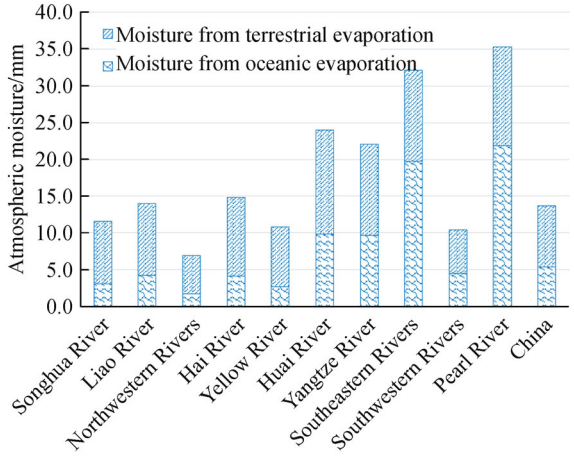

Fig. 5 Atmospheric moisture originating from ocean and land over the ten major river basins in China.

precipitation over China. Precipitation is partitioned into two parts respectively originating from oceanic and terrestrial evaporation. The precipitation over China and the contributions of oceanic and terrestrial evaporation are evaluated. The upper part of Fig. 6 presents the mean annual precipitation from 1980 to 2010. The lower part of Fig. 6 illustrates the contribution (in percentage) of oceanic evaporation. Comparing the upper parts of Fig. 6 and Fig. 3, precipitation exhibits larger regional variability compared with atmospheric moisture. This phenomenon is due to the fact that precipitation is subject to more influencing factors, which include not only atmospheric moisture (precipitable water), but also topography, land use, weather conditions, etc. On the other hand, the contributions of oceanic evaporation to atmospheric moisture and precipitation are quite similar, as illustrated in the lower parts of Fig. 6 and Fig. 3. It is observed that oceanic evaporation contributes more to precipitation in South and East China, whereas terrestrial evaporation makes a greater contribution in Northwest China.

The monthly mean contributions of oceanic and terrestrial evaporation to precipitation for the ten river basins are evaluated, as shown in Fig. 7. Generally, precipitation over China's major river basins exhibits peak values in the summer months. This pattern coincides with the rainy season in the Northern Hemisphere and also the occurrence of the EAM (Ding and Chan, 2005; Huang and Chen, 2010; Li et al., 2011). There are four river basins by the sea in East China (Fig. 4). From south to north, they are the Pearl River, the southeastern rivers, the Huai River, and the Hai River. On the right-hand side of Fig. 7, the four rivers are illustrated from the bottom up. As can be seen, for the Pearl River and the southeastern rivers, oceanic evaporation makes a greater contribution to precipitation than terrestrial evaporation does for the whole year, particularly in the summer months. For the Huai River, oceanic evaporation has a larger contribution in the summer months, while terrestrial evaporation contributes more in the other months. For the Hai River, terrestrial evaporation makes a greater contribution to precipitation for the whole year. This finding is in accordance with earlier findings that the EAM weakens as it advances northward and northeastward in China (Wang and Lin, 2002; Ding and Chan, 2005). In the basins of the Yangtze River and the Southwestern Rivers, the contributions of oceanic and terrestrial evaporation to precipitation are similar in the summer months, but terrestrial evaporation contributes more in the other months. For the Yellow River, the Liao River, the Songhua River, and the northwestern rivers, terrestrial evaporation has a larger contribution to precipitation for the whole year. Particularly for the northwestern rivers, oceanic evaporation exhibits a small contribution for the whole year, due to the dominant effect of westerly wind (Qian et al., 2009; van der Ent et al., 2010).

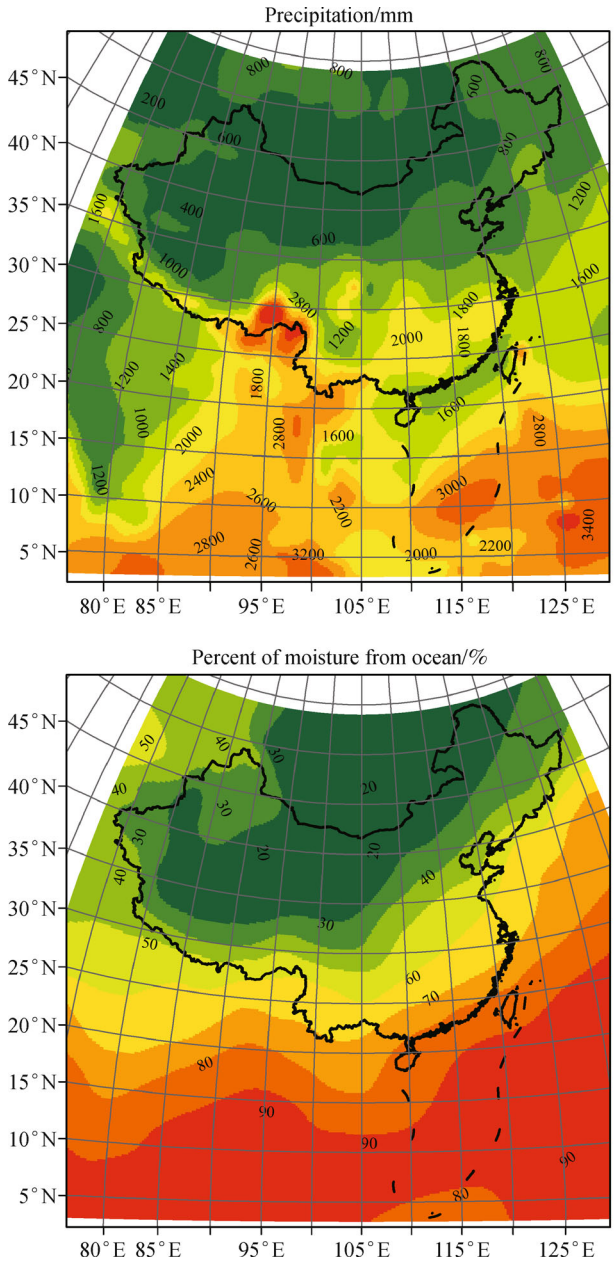

Fig. 6 Mean annual precipitation over China (from 1980 to 2010) and the contribution of oceanic evaporation.

Through the analysis of the source of precipitation over China, this study obtains the following results: the mean annual precipitation over China is 737 mm; 318 mm of the precipitation originates from oceanic evaporation, accounting for 43%; and 420 mm is from terrestrial evaporation, accounting for 57%. Van der Ent et al. (2010) observed the significant effect of the westerly wind in North China. This study also highlights the effect of the westerly wind. Particularly, the westerly wind has a dominant effect on atmospheric moisture and precipitation in Northwest China. On the other hand, the EAM plays a key role, bringing oceanic evaporation and making great contributions to precipitation in South and East China. The estimation of contributions of oceanic and terrestrial evaporation in this study exhibits some differences from the earlier estimation that up to 80% of precipitation over China originates from evaporation from the Eurasian continent (van der Ent et al., 2010; Gimeno et al., 2012; Keys et al., 2012). The different results are due to differences in study regions and atmospheric circulation patterns.

Van der Ent et al. (2010) and Keys et al. (2012) examined the whole Eurasian Continent and observed the significant effect of the westerly wind, which resulted in the estimation that terrestrial evaporation originating from the continent contributes to up to 80% of China's water resources. On the other hand, the westerly wind prevails in the winter months, which is the dry season (Fig. 7). During the summer months, the EAM exhibits extensive influences and transports a great amount of oceanic moisture to East Asia. The rainy season caused by the EAM is called Meiyu in China, Baiu in Japan, and Changma in Korea. Ding and Chan (2005) summarized the onset and seasonal march of the monsoon precipitation in China, Japan, and Korea. The rainy season coincides with the EAM season in China (Qian and Lee, 2000; Wang and Lin, 2002; Ding and Chan, 2005). In a recent study of global water vapor transport, Zahn and Allan (2013) observed significant moisture transport along the coastline in Southeast China, which is closely related to the EAM.

The contributions of oceanic evaporation to precipitation over the ten major river basins are evaluated and shown in Table 3. The river basins are ranked in order from the highest to the lowest. They are the southeastern rivers (67%), the Pearl River (65%), the Huai River (51%), the Yangtze River (46%), the southwestern rivers (43%), the Liao River (37%), the Hai River (32%), the Songhua River (30%), the Yellow River (27%), and the northwestern rivers (25%). The relationship between the mean annual precipitation and the contribution of oceanic evaporation to precipitation is illustrated with a scatter plot in Fig. 8. As can be seen, there is a significant linear relationship, with a correlation coefficient as high as 0.92. It is observed that rivers in the top right corner are located in South and East China, where the climate is subject to the EAM. On the other hand, rivers in the lower left corner are located in North China where the climate is generally dominated by the westerly wind. This figure highlights the joint effects of the EAM and the westerly wind on precipitation over China's major river basins.

6 Summary

This study presents a comprehensive analysis of the source of atmospheric moisture and precipitation over China. It is estimated that from 1980 to 2010, the mean annual atmospheric moisture is 13.7 mm, of which 39% originates

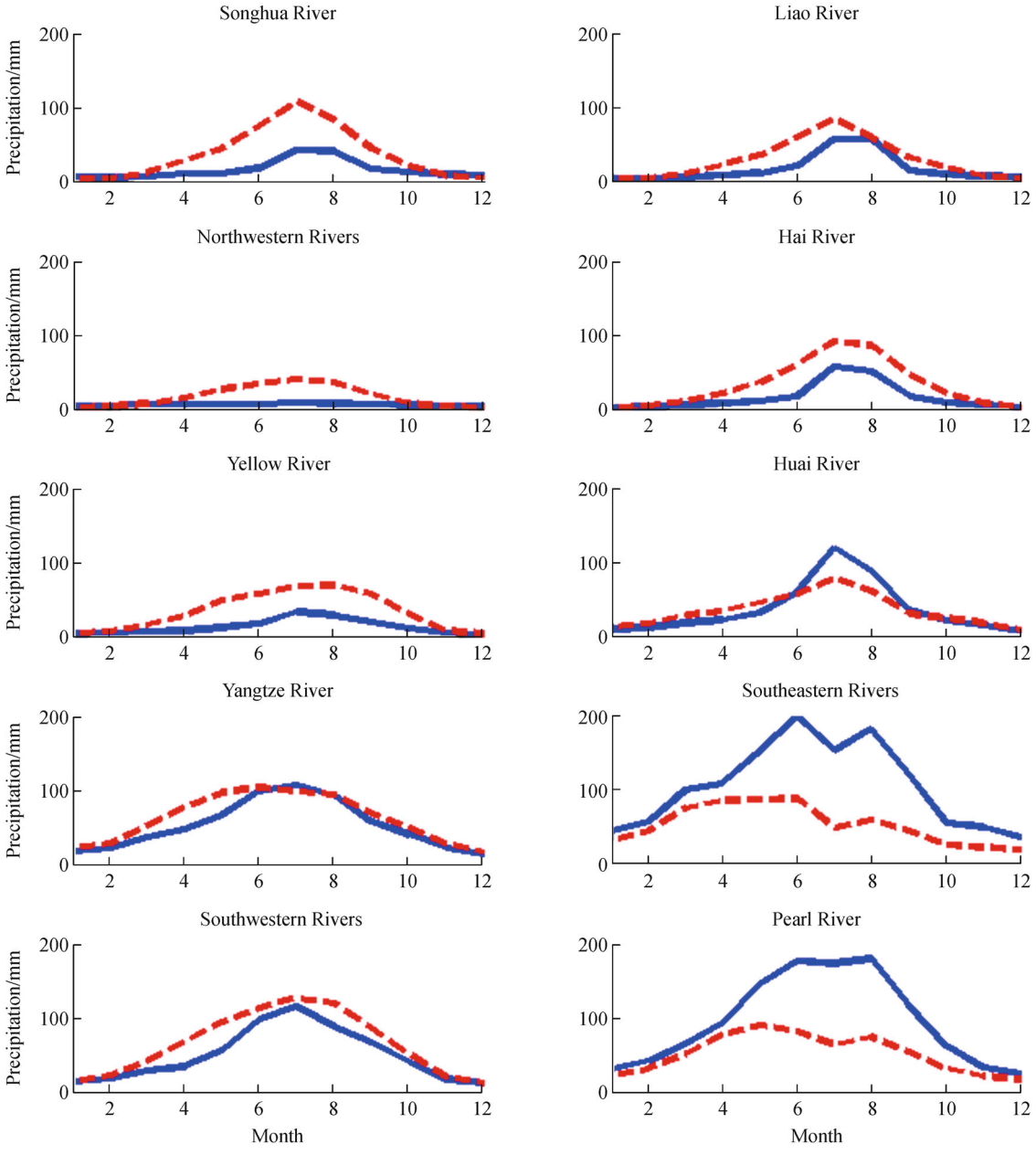

Fig. 7 Annual cycle of oceanic and terrestrial evaporation to precipitation over the ten major river basins in China (the red dashed line represents the contribution of terrestrial evaporation; the blue solid lines indicates the contribution of oceanic evaporation).

from oceanic evaporation and 61% from terrestrial evaporation; the mean annual precipitation is 737 mm, of which 43% is from oceanic evaporation and 57% from terrestrial evaporation. The source of atmospheric moisture and precipitation varies considerably across China due to the different atmospheric circulation patterns. For the Pearl River and the southeastern rivers, oceanic evaporation contributes to more than 60% of atmospheric moisture and precipitation. This result is due to climate in Southeast China being dominated by the EAM, which delivers a large amount of oceanic evaporation to China. In contrast, for the Yellow River and the northwestern rivers, terrestrial evaporation makes a greater contribution to atmospheric moisture and precipitation than oceanic evaporation does. This outcome is attributed to the westerly wind that dominates the climate in Northwest China. It is pointed out that rivers there receive more than 70% of atmospheric moisture and precipitation from evaporation originating from the Eurasian continent.

This study conducts an analysis of sources of atmospheric moisture and precipitation over China. The analysis links the source of atmospheric moisture and

Table 3 Contribution of oceanic and terrestrial evaporation to precipitation over China

Location	Precipitation from oceanic evaporation/mm	Precipitation from terrestrial evaporation/mm	Total precipitation /mm	% from oceanic evaporation	% from terrestrial evaporation
Songhua River	183	431	614	30	70
Liao River	200	339	539	37	63
Northwestern Rivers	63	191	255	25	75
Hai River	181	386	567	32	68
Yellow River	143	390	533	27	73
Huai River	436	413	849	51	49
Yangtze River	610	724	1,335	46	54
Southeastern Rivers	1,258	625	1,883	67	33
Southwestern Rivers	571	755	1,326	43	57
Pearl River	1,132	598	1,730	65	35
China	318	420	737	43	57

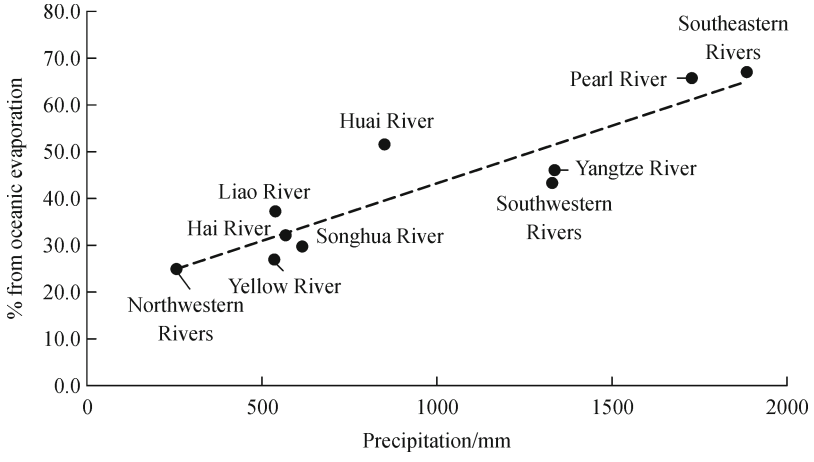

Fig. 8 The correlation relation between mean annual precipitation and the contribution of oceanic evaporation to precipitation for the 10 major river basins in China.

precipitation to atmospheric circulation patterns. In the future, more efforts can be devoted to investigations of hydro-climatic teleconnections, identifying climatic indices that characterize the EAM and the westerly wind, and identifying the relationships between anomalies of climatic indices and precipitation. The teleconnections are expected to enhance seasonal prediction of precipitation. Particularly, the ability to improve the predictability of extreme events of flood and drought is of great importance. Incorporating seasonal predictions into water resources management will lead to improved management of water supply and hydropower, and mitigation of flooding and drought risks.

Acknowledgements The authors would like to thank Dr. Ruud van der Ent for helping to set up the water accounting model, and Prof. Glenn Patterson, Mr. Ragai Wanis and Dr. Junmei Lv for the helpful comments to improve the paper. The research has been financially supported by the National Natural Science Foundation of China (Grant Nos. 51409145 and 51179085) and the National Basic Research Program of China (Nos. 2011BAC09B07 and 2013BAB05B03).

References

Chen Z S, Chen Y N (2014). Effects of climate fluctuations on runoff in the headwater region of the Kaidu River in northwestern China. Front Earth Sci, 8(2): 309–318

Dee D P, Uppala S M, Simmons A J, Berrisford P, Poli P, Kobayashi S, Andrae U, Balmaseda M A, Balsamo G, Bauer P, Bechtold P, Beljaars A C M, van de Berg L, Bidlot J, Bormann N, Delsol C, Dragani R, Fuentes M, Geer A J, Haimberger L, Healy S B, Hersbach H, Hólm E V, Isaksen L, Kållberg P, Köhler M, Matricardi M, McNally A P, Monge-Sanz B M, Morcrette J J, Park B K, Peubey C, de Rosnay P, Tavolato C, Thépaut J N, Vitart F (2011). The ERA-Interim reanalysis: configuration and performance of the data assimilation system. Q J R Meteorol Soc, 137(656): 553–597

Ding Y H, Chan J C L (2005). The East Asian summer monsoon: an overview. Meteorol Atmos Phys, 89(1–4): 117–142

Gevorgyan A (2013). Verification of daily precipitation amount forecasts in Armenia by ERA-Interim model. Int J Climatol, 33(12): 2706–2712

Gimeno L, Stohl A, Trigo R M, Dominguez F, Yoshimura K, Yu L, Drumond A, Durán-Quesada A M, Nieto R (2012). Oceanic and terrestrial sources of continental precipitation. Rev Geophys, 50, RG4003, doi: 10.1029/2012RG000389

Gimeno L, Drumond A, Nieto R, Trigo R M, Stohl A (2010). On the origin of continental precipitation. Geophys Res Lett, 37, L13804, doi: 10.1029/2010GL043712

Huang R, Chen J (2010). Characteristics of the summertime water vapor transports over the eastern part of China and those over the western part of China and their difference. Chinese Journal of Atmospheric Sciences, 34(6): 1035–1046,

Keys P W, van der Ent R J, Gordon L J, Hoff H, Nikoli R, Savenije H H G (2012). Analyzing precipitationsheds to understand the vulnerability of rainfall dependent regions. Biogeosciences, 9(2): 733–746

Li Q, Wei F Y, Li D L (2011). Interdecadal variation of East Asian summer monsoon and drought/flood distribution over eastern China in the last 159 years. J Geogr Sci, 21(4): 579–593

Liu F, Chen S L, Dong P, Peng J (2012). Spatial and temporal variability of water discharge in the Yellow River Basin over the past 60 years. J Geogr Sci, 22(6): 1013–1033

Oki T, Kanae S (2006). Global hydrological cycles and world water resources. Science, 313(5790): 1068–1072

Qian W H, Ding T, Hu H R, Lin X, Qin A M (2009). An overview of dry-wet climate variability among monsoon-westerly regions and the monsoon northernmost marginal active zone in China. Adv Atmos Sci, 26(4): 630–641

Qian W H, Lee D K (2000). Seasonal march of Asian summer monsoon. Int J Climatol, 20(11): 1371–1386

Sun B, Wang H J (2013). Water vapor transport paths and accumulation during widespread snowfall events in northeastern China. J Clim, 26 (13): 4550–4566

Trenberth K E, Smith L, Qian T T, Dai A, Fasullo J (2007). Estimates of the global water budget and its annual cycle using observational and model data. J Hydrometeorol, 8(4): 758–769

van der Ent R J, Savenije H H G (2011). Length and time scales of atmospheric moisture recycling. Atmos Chem Phys, 11(5): 1853–1863

van der Ent R J, Savenije H H G (2013). Oceanic sources of continental precipitation and the correlation with sea surface temperature. Water Resour Res, 49(7): 3993–4004

van der Ent R J, Savenije H H G, Schaefli B, Steele-Dunne S C (2010). Origin and fate of atmospheric moisture over continents. Water Resour Res, 46, W09525, doi: 10.1029/2010WR009127

Wang B, Lin H (2002). Rainy season of the Asian-Pacific summer monsoon. J Clim, 15(4): 386–398

Wei J F, Dirmeyer P A, Bosilovich M G, Wu R G (2012). Water vapor sources for Yangtze River Valley rainfall: climatology, variability, and implications for rainfall forecasting. J Geophys Res, D, Atmospheres, 117(D5), doi: 10.1029/2011JD016902

Wilby R L, Wedgbrow C S, Fox H R (2004). Seasonal predictability of the summer hydrometeorology of the River Thames, UK. J Hydrol (Amst), 295(1–4): 1–16

Xu K, Zhu C W, He J H (2013). Two types of El Nio-related Southern Oscillation and their different impacts on global land precipitation. Adv Atmos Sci, 30(6): 1743–1757

Zahn M, Allan R P (2013). Quantifying present and projected future atmospheric moisture transports onto land. Water Resour Res, 49 (11): 7266–7277

Zhao R X, Zhang H, Wu G X, Li W P, Shi A L (2012). Decadal variations in the season advancement of spring water cycle over Eastern China. Science China Earth Sciences, 55(8): 1358–1370

Zhou M Z, Wang H J, Yang S, Fan K (2013). Influence of springtime North Atlantic Oscillation on crops yields in Northeast China. Clim Dyn, 41(11–12): 3317–3324